JACS
JOURNAL OF THE AMERICAN CHEMICAL SOCIETY
pubs.acs.org/JACS
Communication

Segmental Dynamics of Membranous Cholesterol are Coupled

Lisa A. Della Ripa, Joseph M. Courtney, Samantha M. Phinney, Collin G. Borcik, Martin D. Burke,* Chad M. Rienstra,* and Taras V. Pogorelov*

Cite This: J. Am. Chem. Soc. 2023, 145, 15043−15048
Read Online
ACCESS | Metrics & More | Article Recommendations | Supporting Information

ABSTRACT: Cholesterol promotes the structural integrity of the fluid cell membrane and interacts dynamically with many membrane proteins to regulate function. Understanding site-resolved cholesterol structural dynamics is thus important. This long-standing challenge has thus far been addressed, in part, by selective isotopic labeling approaches. Here we present a new 3D solid-state NMR (SSNMR) experiment utilizing scalar $^{13}C-^{13}C$ polarization transfer and recoupling of the $^{1}H-^{13}C$ interactions in order to determine average dipolar couplings for all $^{1}H-^{13}C$ vectors in uniformly ^{13}C-enriched cholesterol. The experimentally determined order parameters (OP) agree exceptionally well with molecular dynamics (MD) trajectories and reveal coupling among several conformational degrees of freedom in cholesterol molecules. Quantum chemistry shielding calculations further support this conclusion and specifically demonstrate that ring tilt and rotation are coupled to changes in tail conformation and that these coupled segmental dynamics dictate the orientation of cholesterol. These findings advance our understanding of physiologically relevant dynamics of cholesterol, and the methods that revealed them have broader potential to characterize how structural dynamics of other small molecules impact their biological functions.

Coupled structural dynamics play a critical role in protein function,[1−3] and advances in understanding such phenomena reveal new opportunities for next generation rational drug design.[4,5] Similar dynamics likely also play a role in the functions of many biologically active small molecules.[6] But this area has been relatively underdeveloped, and tools for interrogating small molecule dynamics in biologically relevant settings are lacking. These limitations are reflected in the longstanding challenge of understanding the dynamics of cholesterol (Chol) (Figure 1E), one of the most important small molecules in mammalian physiology.

Chol is also very important in human medicine. High levels increase the risk of heart disease, and cholesterol biosynthesis inhibitors can mitigate these risks.[7−9] Dose-limiting renal toxicity of the clinically vital antifungal drug amphotericin B (AmB) requires cholesterol binding,[10,11,14] and AmB analogs with greater selectivity for binding ergosterol relative to Chol have improved therapeutic indices in preclinical studies.[12,13] Chol also plays an important role in the capacity of AmB ion channels to serve as molecular prosthetics for missing or dysfunctional CFTR anion channels. Chol also plays a key role in viral infectivity; for example, HIV fusion peptides preferentially target Chol-rich membrane regions.[14] Chol interactions with proteins such as α-synuclein[15] and β-amyloid[16] are postulated to be critical to regulation of protein aggregation in Parkinson's and Alzheimer's diseases.[16,17]

Chol dynamics in living systems have been the subject of intense study, but insights have been slow to emerge. Sterol lateral mobility has been studied by fluorescence microscopy, but these studies are limited by the potential artifactual effects of the chemical modifications. Experiments combining site-specific deuterium (^{2}H) labeling with SSNMR spectroscopy can measure the magnitude and time scale of molecular motions in phospholipid bilayers. These properties are reported in OP[18−21] and quadrupolar relaxation rates,[22] respectively, and are used to quantify Chol modulation of membrane fluidity as a function of composition and temperature.[23] A ^{2}H SSNMR spectroscopy-based study demonstrated that the acyclic aliphatic tail, but not the fused tetracyclic core, of Chol contributes to membrane condensation.[24] Intermolecular $^{13}C-^{19}F$ REDOR distances identified the Chol-binding motifs in M2 underlying the mechanism of membrane scission in budding virus cells.[25] These studies are currently limited in both efficiency and resolution due to their dependence on site-specific labeling.

A roadmap for addressing these limitations has been laid in recent studies of the structures and dynamics of membrane and fibrous proteins, leveraging combined uniform isotopic enrichment, high magnetic fields, and state-of-the-art SSNMR methods.[26−33] These powerful strategies have been proven useful for more illuminating functionally relevant interactions of Chol with membrane proteins.[34−36] Here we employed a combination of uniformly labeled Chol (U-^{13}C-Chol), new 3D SSNMR experiments that utilize scalar $^{13}C-^{13}C$ polarization transfer and recoupling of the $^{1}H-^{13}C$ interactions to determine average dipolar couplings for all $^{1}H-^{13}C$ vectors, and multilevel theory including all-atom MD simulations and QM calculations to illuminate the structure and dynamics of Chol in membrane with heightened resolution. We reveal that

Received: March 28, 2023
Published: July 6, 2023

https://doi.org/10.1021/jacs.3c01775
J. Am. Chem. Soc. 2023, 145, 15043−15048

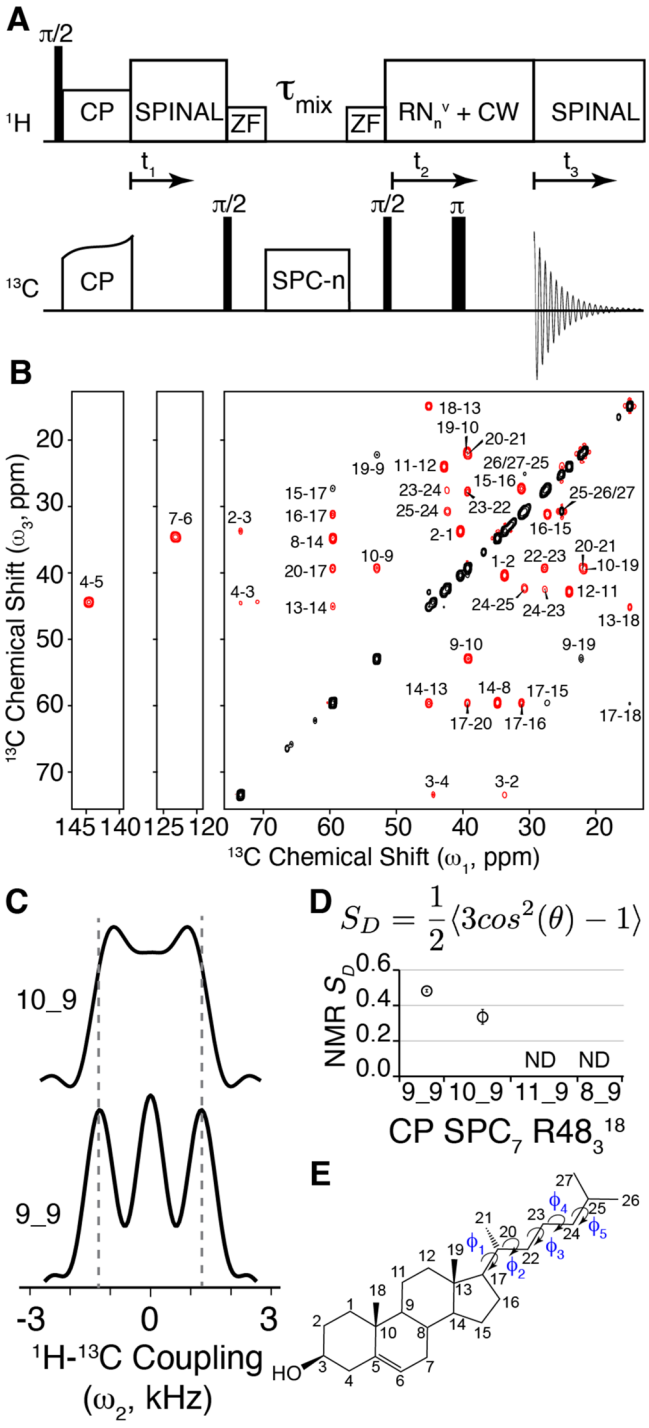

Figure 1. (A) CP-SPCn-RNnv pulse sequence. (B) 600 MHz SSNMR $^{13}C-^{13}C$ spectrum with 1.44 ms SPC9 mixing of a 10:3 POPC:U-^{13}C-Chol sample at 20 °C, collected at 11.111 kHz. (C) Lineshapes extracted from C10−C9 and C9 diagonal peaks. (D) NMR OP, S_D, defined, and C9 OP extracted from a CP-SPC7-R48$_3^{18}$ experiment. (E) Cholesterol molecular structure. The 1D ^{13}C CP spectrum is shown in Figure S1.

the segmental dynamics of Chol in palmitoyloleoylphosphatidylcholine (POPC) membranes are coupled, and such coupling dictates the orientation.

We first attempted to measure the $^1H-^{13}C$ dipolar couplings using a fully dipolar 3D R-symmetry[37,38] experiment (Figure 1A), which recouples heteronuclear but decouples homonuclear couplings. The SSNMR experiments place the chemical shifts of the $^{13}C-^{13}C$ correlation into the $\omega_1-\omega_3$ dimensions and the C−H dipolar coupling in the ω_2 dimension and correspond to the C−H dipolar coupling of the ^{13}C site along the ω_1 axis. We used $^1H-^{13}C$ cross-polarization (CP) and $^{13}C-^{13}C$ SPCn mixing[39] to achieve signal enhancement and dipolar mixing, respectively. The resulting CP-SPCn-RN$_n^\nu$ 3D spectrum exhibited some surprising spectral features. First, several one-bond correlations are missing. For example, the 2D SPCn spectrum in Figure 1B lacks correlations between C11−C9 and C8−C9. Second, several peaks are asymmetric across the diagonal, such as C25−C26 and C9−C10. Third, for several sites the two-bond correlations are stronger than one-bond correlations. For example, it is particularly striking in Figure 1B how weak the C2−C3 and C4−C3 correlations are compared to other one-bond correlations. Having precisely assessed the site-specific ^{13}C-labeling percentages previously,[40] we focus our attention on the spectroscopic origins of these surprising results.

A major advantage of 3D SSNMR is that each data set contains an abundance of internal controls to confirm that the experiment and sample remain stable throughout data collection. For Chol, multiple peaks report on the same heteronuclear dipolar coupling; e.g, the C9−C9, C8−C9, C10−C9, and C11−C9 ($\omega_1-\omega_3$) cross- and autocorrelation peaks all report on (multiple) $^1H-^{13}C$ dipolar couplings to the C9 site, and the (in)consistency of the obtained OP (in)validates the resulting interpretation. The fully dipolar experiment yielded systematic differences in the dipolar line shape data (Figure 1C) and the fitted OP (Figure 1D). Extreme examples of this—where the dipolar vectors lie near the magic angle relative to the motional axis, such as C11−C9 and C8−C9—show nearly complete averaging of the couplings and therefore peaks with marginal signal-to-noise (SNR) ratios. We hypothesized that the differences among these sites, both in the data quality and resulting fits, arose due to the orientational dependence of the $^1H-^{13}C$ and $^{13}C-^{13}C$ dipolar couplings responsible for transferring polarization to each ^{13}C site in $\omega_1-\omega_3$ respectively. If correct, such effects can be a powerful way to probe the molecular orientation. To test this hypothesis, we interrogated if these effects on the heteronuclear dipolar coupling measurements would be negated if we implemented a direct polarization (DP) COSY R-symmetry or fully scalar (through-bond) scheme. We developed a version of the pulse sequence comprising ^{13}C DP followed by polarization transfer using the CTUC−COSY mixing scheme,[41] followed by the same type of R-symmetry heteronuclear recoupling (Figure 2A).[42] The spectrum derived from this DP-COSY-RN$_n^\nu$ sequence has sensitivity higher than that of the CP-SPCn-RN$_n^\nu$ dipolar version and reports only on the one-bond correlations under the conditions employed here. Supporting our hypothesis, the DP-COSY-RN$_n^\nu$ experiment yielded consistent OP derived from all correlations (Figure 2C, 2D), including those of C9 where the C8−C9 and C11−C9 peaks were absent from the fully dipolar spectrum. Multiple OP determinations from the same spectrum increased the robustness and precision of these measurements, and we thus obtained a highly confident experimental OP for the entire Chol molecule.

The OP obtained from MD simulations (Figure 3A) of Chol in a POPC membrane (Figure 3B) agreed with the experimental data (Figures 3C, S3), enabling interrogation of

https://doi.org/10.1021/jacs.3c01775
J. Am. Chem. Soc. 2023, 145, 15043−15048

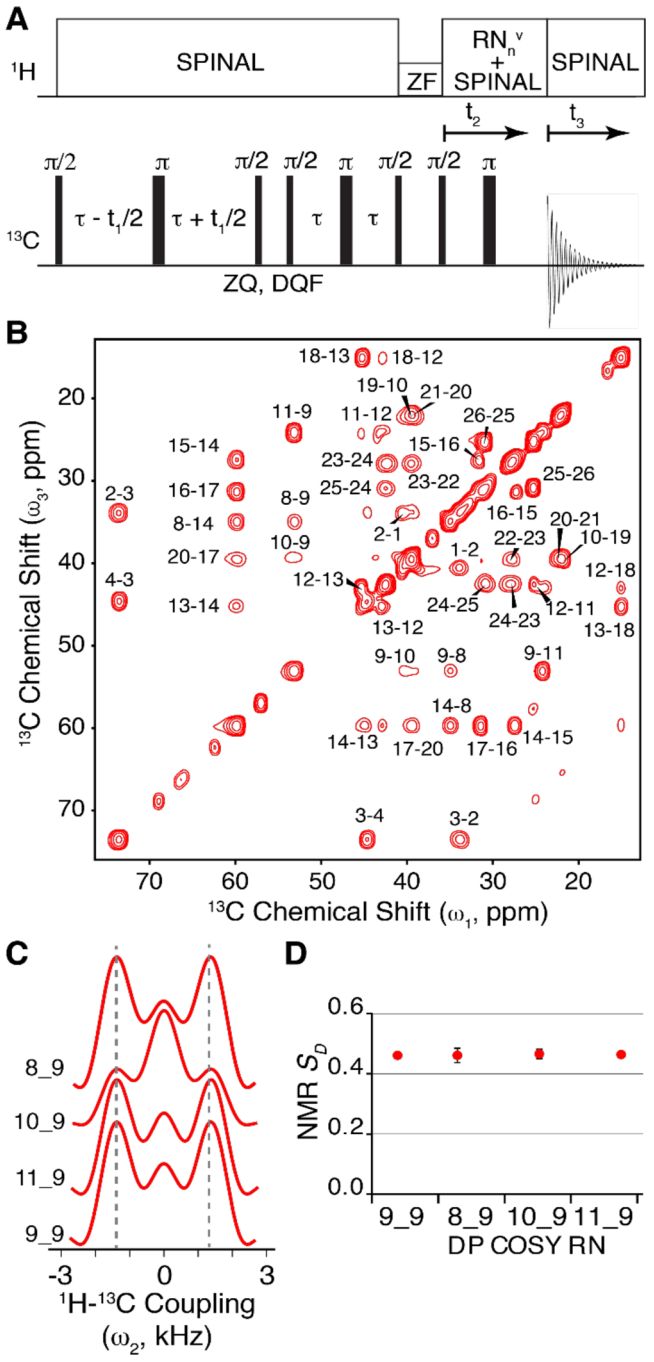

Figure 2. (A) DP-COSY-RNnv pulse sequence. (B) $^{13}C-^{13}C$ 2D plane of DP-COSY-R18$_1^7$ 3D. (C) Dipolar lineshapes from a fully scalar version of the RNnv pulse sequence used to measure OP. Gray dotted lines are used to guide the eyes to evaluate the dipolar couplings. (D) OP collected under DP-COSY-R18$_1^7$, show consistency between those measured with a fully scalar pulse sequence and elimination of the orientational dependence on dipolar transfer. The temperature of the sample has minimal effects on the dipolar order parameter (Figure S13).

the results of the MD. We expand upon the agreement of SSNMR to MD OP in the supplementary text.

In addition to the extraction of OP which report on the rotational motion of a bond vector, temporal and spatial resolution of all-atom MD simulations enabled reporting on the dynamic chemical environment of membranous Chol.[21,24] Our MD simulations revealed the preferred conformations

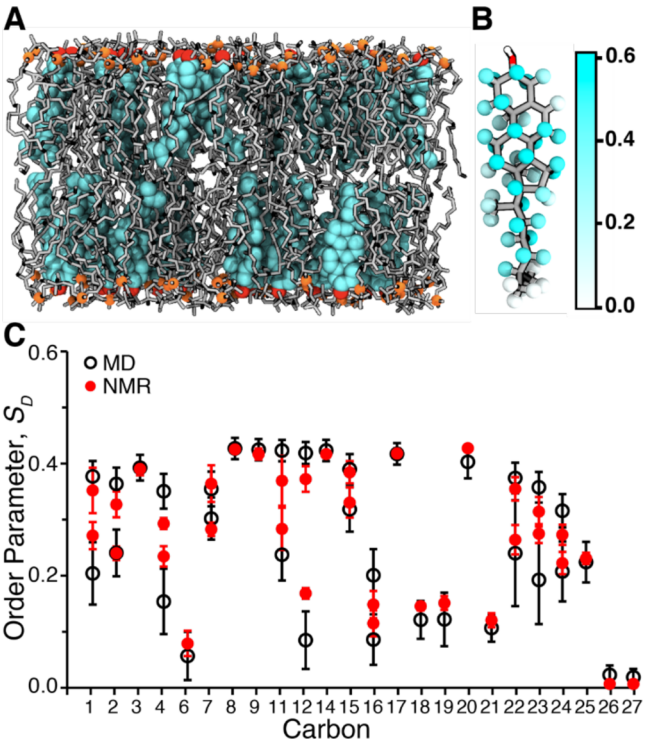

Figure 3. (A) Membrane-sterol MD model of 300 cholesterol molecules (cyan) modeled in 10 10:3 POPC:Chol replicates and sampled at 100 ns. POPC lipids (gray). (B) Chol protons color-coded by MD S$_D$. (C) NMR and MD OP comparison.

sampled by the Chol tails (Figure 4). We define the five tail dihedral angles $\varphi_1-\varphi_5$ (Figures 4A, S5), and as expected, φ_1 mostly samples the *gauche* conformation (Figure 4A), to minimize the steric clash that occurs between the C21 and C18 methyl groups. On the other hand, the φ_5 is equally sampling the *gauche* and *trans* conformations, in agreement with the single peak for C26 and C27 in the NMR spectrum. The other dihedral angles primarily adopt *trans* conformations. These findings agree with previous computational studies,[21,24] and our calculated CS distributions agree with SSNMR-measured shifts (Figures S4, S6, S7).

We examined the CS agreement using the RMSD between the SSNMR and MD-based QM by gradually increasing the xtxxx population of $\varphi_1-\varphi_5$ angles from 0% to 100%, in the background of the xgxxx population, where x is either *gauche* or *trans* (Figure 4B). The experimental and calculated CS as a function of φ_2 conformation revealed that, for the best agreement, ~70% of the Chol tails have to be in a *trans* φ_2 dihedral conformation in POPC membranes in the liquid phase. Remarkably, our approach provided insight into the preferred conformations of the Chol tails in the SSNMR sample. By this metric, our MD simulations agree well with the experimental data, as a larger portion of the Chols (61%) had a *trans* φ_2 conformation which is within the accuracy of this study (Figure 4B). We suggest that the approach outlined here in principle can be used for future improvements in force fields.

We then used the MD of tail dihedral angles and Chol tilt and rotation to gain insights into the Chol dynamics within the membrane. Using cross-correlation analysis of tail dihedral angles and molecular motions (see Table S1) we revealed coupled dynamics of membranous Chol. Specifically, there are

https://doi.org/10.1021/jacs.3c01775
J. Am. Chem. Soc. 2023, 145, 15043−15048

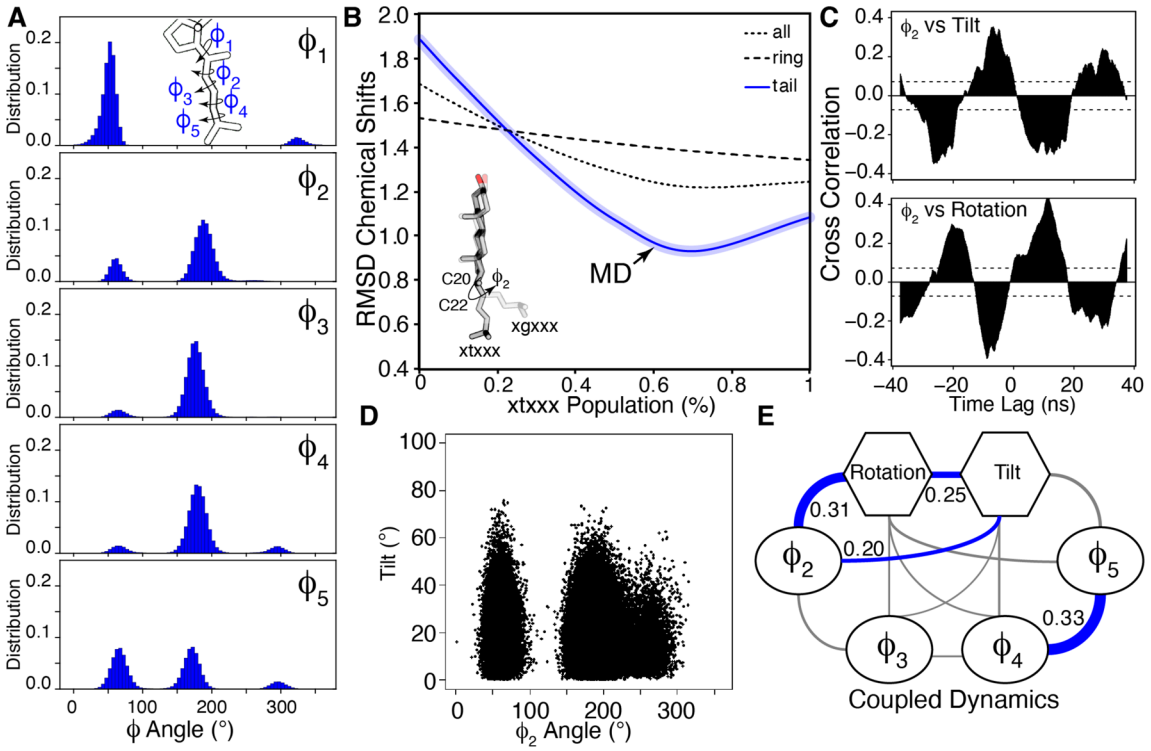

Figure 4. (A) Tail dihedral angle populations in MD simulations. (B) RMSD between SSNMR chemical shifts and scaled shieldings as a function of xtxxx population, bandwidth (blue) indications uncertainty. The MD xtxxx population is 61% (black arrow). (C) Cross-correlations of φ_2 to tilt and axial rotation. (D) φ_2 versus tilt. (E) Coupled segmental dynamics with all significant couplings (cross-correlation) shown (blue).

significant correlations between φ_2 and both the tilt angle and axial rotation of Chol as well as anticorrelation between the latter (Figures 4C, S8–S9). Our approach also shows that, as expected from their geometry, the dynamics of the highly mobile φ_4 and φ_5 are positively correlated, and importantly, the strength of their coupling, 0.33 (Figure 4E), can serve as a basis for comparison for other values. The Chol dynamics and that of its tail are correlated, as φ_2 influences the rotation and tilt of the whole molecule. Appropriately, the MD lifetimes of these three processes are similar (Figure S11). Intriguingly, a previous computational study[45] suggested the importance of the C21 methyl group, the node between φ_1 and φ_2, in maintaining optimal Chol tilt. Further analysis of the tail dihedral angles using a Markov model revealed that a direct *gauche* to *trans* transition of φ_2 was rarely observed in simulations and that a plausible pathway needs to involve changes in dihedral angles downstream of φ_2—in a "crankshaft manner" (Figure S11, Table S2). The direct transition from *gauche* to *trans* for φ_2 may require a large motion of the tail while in close proximity to lipid tails as well as neighboring Chol[46] molecules. In fact, in agreement with a recent study,[47] our MD simulations also revealed formation of Chol oligomers (Figure S12) that allow a limited space for rearrangements. Overall, our data revealed that tail dihedral angle φ_2 plays a key role in Chol's dynamics.

Through combination of new SSNMR experiments on highly enriched U-^{13}C-Chol and all-atom MD simulations in combination with QM calculations, it was possible to resolve coupled dynamics of Chol in lipid bilayers. The development of a fully scalar 3D pulse sequence allowed for precise and consistent collection of OP at each site throughout the Chol molecule. The OP extracted from the MD simulations matched the experimental results. The direct connection of experimental and simulations results allowed us to determine the actual tail conformations present in the experimental sample, and multiple lines of analysis revealed coupled segmental dynamics. Chol tails impact motions of the whole molecules. We are intrigued by the future opportunities that this unique combination of methodologies has opened to study Chol influence on functional dynamics of proteins and small molecule drug targets.

■ ASSOCIATED CONTENT

Supporting Information

The Supporting Information is available free of charge at https://pubs.acs.org/doi/10.1021/jacs.3c01775.

Detailed analyses, spectral data, and method descriptions. (PDF)

■ AUTHOR INFORMATION

Corresponding Authors

Chad M. Rienstra − *Department of Biochemistry, National Magnetic Resonance Facility at Madison, and Morgridge Institute for Research, University of Wisconsin—Madison, Madison, Wisconsin 53706, United States;* orcid.org/0000-0002-9912-5596; Email: crienstra@wisc.edu

Martin D. Burke − *Department of Chemistry, Department of Biochemistry, Beckman Institute for Advanced Science and Technology, and Carle Illinois College of Medicine, University of Illinois at Urbana—Champaign, Urbana, Illinois 61801, United States;* orcid.org/0000-0001-7963-7140; Email: mdburke@illinois.edu

Taras V. Pogorelov − *Department of Chemistry, Center for Biophysics and Quantitative Biology, School of Chemical Sciences, National Center for Supercomputing Applications,*

https://doi.org/10.1021/jacs.3c01775
J. Am. Chem. Soc. 2023, 145, 15043−15048

and Beckman Institute for Advanced Science and Technology, University of Illinois at Urbana—Champaign, Urbana, Illinois 61801, United States; orcid.org/0000-0001-5851-7721; Email: pogorelo@illinois.edu

Authors

Lisa A. Della Ripa − *Department of Chemistry, University of Illinois at Urbana—Champaign, Urbana, Illinois 61801, United States*

Joseph M. Courtney − *Department of Chemistry, University of Illinois at Urbana—Champaign, Urbana, Illinois 61801, United States*

Samantha M. Phinney − *Department of Biochemistry, University of Illinois at Urbana—Champaign, Urbana, Illinois 61801, United States*

Collin G. Borcik − *Department of Biochemistry, University of Wisconsin—Madison, Madison, Wisconsin 53706, United States*

Complete contact information is available at: https://pubs.acs.org/10.1021/jacs.3c01775

Notes

The authors declare no competing financial interest.

■ ACKNOWLEDGMENTS

Authors thank Dr. Evgeny Nimerovsky for coding the fully scalar pulse sequence. We acknowledge the NIH (R01-GM112845, R01-GM123455, R01-GM141298, R35-GM118185, and P41-GM136463) for financial support. L.A.D.R. is supported by the NIH-supported Chemical Biology Interface Training Program (T32-GM070421). C.G.B. is supported by the NIH Ruth L. Kirschstein Fellowship (F32-GM149118). The content is solely the responsibility of the authors and does not necessarily represent the official views of the National Institutes of Health. We are grateful to the Extreme Science and Engineering Discovery Environment (XSEDE, grants TG-MCB130112 (T.V.P.) and MCB150132 (C.M.R. and T.V.P.)), which is supported by National Science Foundation grant number ACI-1053575. Portions of the data appeared in the Ph.D. dissertation of L.A.D.R.

■ REFERENCES

(1) Frauenfelder, H.; Sligar, S.; Wolynes, P. The Energy Landscapes and Motions of Proteins. *Science* **1991**, *254*, 1598−1603.

(2) Lee, A. L.; Wand, A. J. Microscopic Origins of Entropy, Heat Capacity and the Glass Transition in Proteins. *Nature* **2001**, *411*, 501−504.

(3) Agafonov, R. V.; Wilson, C.; Otten, R.; Buosi, V.; Kern, D. Energetic Dissection of Gleevec's Selectivity toward Human Tyrosine Kinases. *Nature Structural and Molecular Biology* **2014**, *21*, 848−853.

(4) Kenakin, T. Theoretical Aspects of GPCR−Ligand Complex Pharmacology. *Chem. Rev.* **2017**, *117*, 4−20.

(5) Stank, A.; Kokh, D. B.; Fuller, J. C.; Wade, R. C. Protein Binding Pocket Dynamics. *Acc. Chem. Res.* **2016**, *49*, 809−815.

(6) Hallock, M. J.; Greenwood, A. I.; Wang, Y.; Morrissey, J. H.; Tajkhorshid, E.; Rienstra, C. M.; Pogorelov, T. V. Calcium-Induced Lipid Nanocluster Structures: Sculpturing of the Plasma Membrane. *Biochemistry* **2018**, *57*, 6897−6905.

(7) Kannel, W. B. Serum Cholesterol, Lipoproteins, and the Risk of Coronary Heart Disease. *Ann. Int. Med.* **1971**, *74*, 1.

(8) Castelli, W. P.; Garrison, R. J.; Wilson, P. W. F.; Abbott, R. D.; Kalousdian, S.; Kannel, W. B. Incidence of Coronary Heart Disease and Lipoprotein Cholesterol Levels: The Framingham Study. *JAMA: The Journal of the American Medical Association* **1986**, *256*, 2835−2838.

(9) Trialists, C. T. Efficacy and Safety of Cholesterol-Lowering Treatment: Prospective Meta-Analysis of Data from 90 056 Participants in 14 Randomised Trials of Statins. *Lancet* **2005**, *366*, 1267−1278.

(10) Anderson, T. M.; Clay, M. C.; Cioffi, A. G.; Diaz, K. A.; Hisao, G. S.; Tuttle, M. D.; Nieuwkoop, A. J.; Comellas, G.; Maryum, N.; Wang, S.; Uno, B. E.; Wildeman, E. L.; Gonen, T.; Rienstra, C. M.; Burke, M. D. Amphotericin Forms an Extramembranous and Fungicidal Sterol Sponge. *Nat. Chem. Biol.* **2014**, *10*, 400−406.

(11) Gray, K. C.; Palacios, D. S.; Dailey, I.; Endo, M. M.; Uno, B. E.; Wilcock, B. C.; Burke, M. D. Amphotericin Primarily Kills Yeast by Simply Binding Ergosterol. *Proc. Natl. Acad. Sci. U. S. A.* **2012**, *109*, 2234−2239.

(12) Wilcock, B. C.; Endo, M. M.; Uno, B. E.; Burke, M. D. C2'-OH of Amphotericin B Plays an Important Role in Binding the Primary Sterol of Human Cells but Not Yeast Cells. *J. Am. Chem. Soc.* **2013**, *135*, 8488−8491.

(13) Endo, M. M.; Cioffi, A. G.; Burke, M. D. Our Path to Less Toxic Amphotericins. *Synlett* **2016**, *27*, 337−354.

(14) Tang, Y.; Leao, I. C.; Coleman, E. M.; Broughton, R. S.; Hildreth, J. E. K. Deficiency of Niemann-Pick Type C-1 Protein Impairs Release of Human Immunodeficiency Virus Type 1 and Results in Gag Accumulation in Late Endosomal/Lysosomal Compartments. *Journal of Virology* **2009**, *83*, 7982−7995.

(15) Leftin, A.; Job, C.; Beyer, K.; Brown, M. F. Solid-State ^{13}C NMR Reveals Annealing of Raft-like Membranes Containing Cholesterol by the Intrinsically Disordered Protein α-Synuclein. *J. Mol. Biol.* **2013**, *425*, 2973−2987.

(16) Barrett, P. J.; Song, Y.; Van Horn, W. D.; Hustedt, E. J.; Schafer, J. M.; Hadziselimovic, A.; Beel, A. J.; Sanders, C. R. The Amyloid Precursor Protein Has a Flexible Transmembrane Domain and Binds Cholesterol. *Science* **2012**, *336*, 1168−1171.

(17) Ji, S. R.; Wu, Y.; Sui, S. F. Cholesterol Is an Important Factor Affecting the Membrane Insertion of β-Amyloid Peptide (AB1−40), Which May Potentially Inhibit the Fibril Formation. *J. Biol. Chem.* **2002**, *277*, 6273−6279.

(18) Oldfield, E.; Chapman, D. Effects of Cholesterol and Cholesterol Derivatives on Hydrocarbon Chain Mobility in Lipids. *Biochemical and biophysical research communications* **1971**, *43*, 610−616.

(19) Matsumori, N.; Kasai, Y.; Oishi, T.; Murata, M.; Nomura, K. Orientation of Fluorinated Cholesterol in Lipid Bilayers Analyzed by ^{19}F Tensor Calculation and Solid-State NMR. *J. Am. Chem. Soc.* **2008**, *130*, 4757−4766.

(20) Shaikh, S. R.; Cherezov, V.; Caffrey, M.; Soni, S. P.; LoCascio, D.; Stillwell, W.; Wassall, S. R. Molecular Organization of Cholesterol in Unsaturated Phosphatidylethanolamines: X-Ray Diffraction and Solid State 2 H NMR Reveal Differences with Phosphatidylcholines. *J. Am. Chem. Soc.* **2006**, *128*, 5375−5383.

(21) Ferreira, T. M.; Coreta-Gomes, F.; Ollila, O. H. S.; Moreno, M. J.; Vaz, W. L. C.; Topgaard, D. Cholesterol and POPC Segmental Order Parameters in Lipid Membranes: Solid State ^{1}H− ^{13}C NMR and MD Simulation Studies. *Physical chemistry chemical physics: PCCP* **2013**, *15*, 1976−1989.

(22) Dufourc, E. J.; Smith, I. C. P. A Detailed Analysis of the Motions of Cholesterol in Biological Membranes by ^{2}H-NMR Relaxation. *Chem. Phys. Lipids* **1986**, *41*, 123−135.

(23) Yeagle, P. L.; Albert, A. D.; Boesze-Battaglia, K.; Young, J.; Frye, J. Cholesterol Dynamics in Membranes. *Biophys. J.* **1990**, *57*, 413−424.

(24) Vogel, A.; Scheidt, H. A.; Baek, D. J.; Bittman, R.; Huster, D. Structure and Dynamics of the Aliphatic Cholesterol Side Chain in Membranes as Studied by ^{2}H NMR Spectroscopy and Molecular Dynamics Simulation. *Phys. Chem. Chem. Phys.* **2016**, *18*, 3730−3738.

(25) Elkins, M. R.; Williams, J. K.; Gelenter, M. D.; Dai, P.; Kwon, B.; Sergeyev, I. V.; Pentelute, B. L.; Hong, M. *Cholesterol-Binding Site of the Influenza M2 Protein in Lipid Bilayers from Solid-State NMR.* Proceedings of the National Academy of Sciences of the United States of America 2017, 201715127.

(26) Tang, M.; Comellas, G.; Rienstra, C. M. Advanced Solid-State NMR Approaches for Structure Determination of Membrane Proteins and Amyloid Fibrils. *Acc. Chem. Res.* **2013**, *46* (9), 2080−2088.
(27) Martin, R. W.; Kelly, J. E.; Kelz, J. I. Advances in Instrumentation and Methodology for Solid-State NMR of Biological Assemblies. *J. Struct. Biol.* **2019**, *206*, 73−89.
(28) Wang, M.; Lu, M.; Fritz, M. P.; Quinn, C. M.; Byeon, I. J. L.; Byeon, C. H.; Struppe, J.; Maas, W.; Gronenborn, A. M.; Polenova, T. Fast Magic-Angle Spinning 19F NMR Spectroscopy of HIV-1 Capsid Protein Assemblies. *Angewandte Chemie - International Edition* **2018**, *57*, 16375−16379.
(29) Prade, E.; Bittner, H. J.; Sarkar, R.; Lopez del Amo, J. M.; Althoff-Ospelt, G.; Multhaup, G.; Hildebrand, P. W.; Reif, B. Structural Mechanism of the Interaction of Alzheimer Disease Aβ Fibrils with the Non-Steroidal Anti-Inflammatory Drug (NSAID) Sulindac Sulfide. *J. Biol. Chem.* **2015**, *290*, 28737−28745.
(30) Potapov, A.; Yau, W. M.; Ghirlando, R.; Thurber, K. R.; Tycko, R. Successive Stages of Amyloid-β Self-Assembly Characterized by Solid-State Nuclear Magnetic Resonance with Dynamic Nuclear Polarization. *J. Am. Chem. Soc.* **2015**, *137*, 8294−8307.
(31) Mukhopadhyay, D.; Gupta, C.; Theint, T.; Jaroniec, C. P. Peptide Bond Conformation in Peptides and Proteins Probed by Dipolar Coupling-Chemical Shift Tensor Correlation Solid-State NMR. *J. Magn. Reson.* **2018**, *297*, 152−160.
(32) Aucoin, D.; Xia, Y.; Theint, T.; Nadaud, P. S.; Surewicz, K.; Surewicz, W. K.; Jaroniec, C. P. Protein-Solvent Interfaces in Human Y145Stop Prion Protein Amyloid Fibrils Probed by Paramagnetic Solid-State NMR Spectroscopy. *J. Struct. Biol.* **2019**, *206*, 36−42.
(33) Zhang, Z.; Liu, H.; Deng, J.; Tycko, R.; Yang, J. Optimization of Band-Selective Homonuclear Dipolar Recoupling in Solid-State NMR by a Numerical Phase Search. *J. Chem. Phys.* **2019**, *150*, 154201.
(34) Borcik, C. G.; Eason, I. R.; Vanderloop, B.; Wylie, B. J. 2H,13C-Cholesterol for Dynamics and Structural Studies of Biological Membranes. *ACS Omega* **2022**, *7*, 17151−17160.
(35) Borcik, C. G.; Eason, I. R.; Yekefallah, M.; Amani, R.; Han, R. X.; Vanderloop, B. H.; Wylie, B. J. A Cholesterol Dimer Stabilizes the Inactivated State of an Inward-Rectifier Potassium Channel. *Angew. Chem. Int. Edit* **2022**, *61*, No. e202112232.
(36) Elkins, M. R.; Sergeyev, I. V.; Hong, M. Determining Cholesterol Binding to Membrane Proteins by Cholesterol ^{13}C Labeling in Yeast and Dynamic Nuclear Polarization NMR. *J. Am. Chem. Soc.* **2018**, *140*, 15437−15449.
(37) Hou, G.; Byeon, I.-J. L. J. L.; Ahn, J.; Gronenborn, A. M.; Polenova, T. ^{1}H− ^{13}C/ ^{1}H− ^{15}N Heteronuclear Dipolar Recoupling by R-Symmetry Sequences Under Fast Magic Angle Spinning for Dynamics Analysis of Biological and Organic Solids. *J. Am. Chem. Soc.* **2011**, *133*, 18646−18655.
(38) Zhao, X.; Eden, M.; Levitt, M. H.; Edén, M.; Levitt, M. H. Recoupling of Heteronuclear Dipolar Interactions in Solid-State NMR Using Symmetry-Based Pulse Sequences. *Chem. Phys. Lett.* **2001**, *342*, 353−361.
(39) Courtney, J. M.; Rienstra, C. M. Efficient Dipolar Double Quantum Filtering under Magic Angle Spinning without a ^{1}H Decoupling Field. *J. Magn. Reson.* **2016**, *269*, 152−156.
(40) Della Ripa, L. A.; Petros, Z. A.; Cioffi, A. G.; Piehl, D. W.; Courtney, J. M.; Burke, M. D.; Rienstra, C. M. Solid-State NMR of Highly ^{13}C-Enriched Cholesterol in Lipid Bilayers. *Methods* **2018**, *138−139*, 47−53.
(41) Chen, L.; Olsen, R. A.; Elliott, D. W.; Boettcher, J. M.; Zhou, D. H.; Rienstra, C. M.; Mueller, L. J. Constant-Time Through-Bond ^{13}C Correlation Spectroscopy for Assigning Protein Resonances with Solid-State NMR Spectroscopy. *J. Am. Chem. Soc.* **2006**, *128*, 9992−9993.
(42) Nimerovsky, E.; Soutar, C. P. A Modification of γ-Encoded RN Symmetry Pulses for Increasing the Scaling Factor and More Accurate Measurements of the Strong Heteronuclear Dipolar Couplings. *J. Magn. Reson.* **2020**, *319*, 106827.
(43) Dufourc, E. J.; Smith, I. C. P. A Detailed Analysis of the Motions of Cholesterol in Biological Membranes by ^{2}H-NMR Relaxation. *Chem. Phys. Lipids* **1986**, *41*, 123−135.
(44) Taylor, M. G.; Akiyama, T.; Smith, I. C. P. The Molecular Dynamics of Cholesterol in Bilayer Membranes: A Deuterium NMR Study. *Chem. Phys. Lipids* **1981**, *29*, 327−339.
(45) Pöyry, S.; Róg, T.; Karttunen, M.; Vattulainen, I. Significance of Cholesterol Methyl Groups. *J. Phys. Chem. B* **2008**, *112*, 2922−2929.
(46) Bandara, A.; Panahi, A.; Pantelopulos, G. A.; Straub, J. E. Exploring the Structure and Stability of Cholesterol Dimer Formation in Multicomponent Lipid Bilayers. *J. Comput. Chem.* **2017**, *38*, 1479−1488.
(47) Elkins, M. R.; Bandara, A.; Pantelopulos, G. A.; Straub, J. E.; Hong, M. Direct Observation of Cholesterol Dimers and Tetramers in Lipid Bilayers. *J. Phys. Chem. B* **2021**, *125*, 1825−1837.

https://doi.org/10.1021/jacs.3c01775
J. Am. Chem. Soc. 2023, 145, 15043−15048